Supporting Information

Electrochemical studies on the permeable characteristics of thiol-modified double-stranded DNA self-assembled monolayers on gold

Zhiguo Li,[a] Tianxing Niu,[a] Zhenjiang Zhang,[a,b] Ran Chen,[a] Guiying Feng,[a] and Shuping Bi* [a]

[a] *School of Chemistry and Chemical Engineering, State Key Laboratory of Coordination Chemistry & Key Laboratory of MOE for Life Science, Nanjing University, Nanjing 210093, China*

[b] *College of Chemistry, Chemical Engineering and Materials Science, Soochow University, Suzhou 215006, China*

Content

1. Molecular structure of thiol-modified double-stranded DNA (HS-$(CH_2)_6$-5'-AGT ACA GTC ATC GCG-3' and complementary chain)

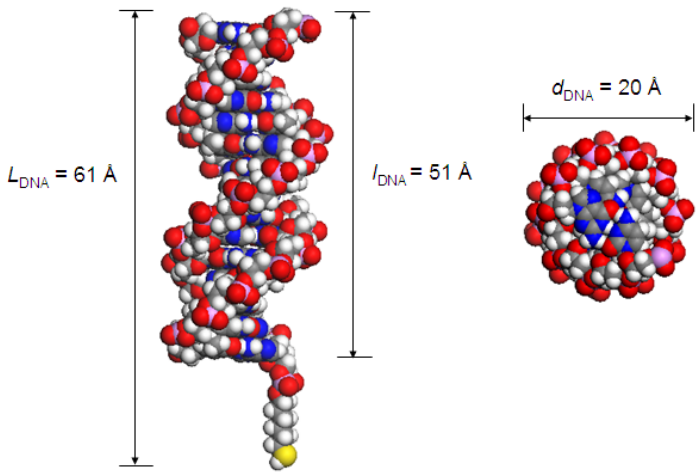

(A) Side view (B) Planform view

Fig. S1 Molecular structure (A, side view; B, planform view) of thiol-modified double-stranded DNA (HS-$(CH_2)_6$-5'-AGT ACA GTC ATC GCG-3' and complementary chain) (drew by Materials Studio software 3.2) [1]. L_{DNA} (the geometrical length of thiol-modified ds-DNA molecule, 61 Å in our study), l_{DNA} (ds-DNA geometrical length, 51 Å in our study) and d_{DNA} (ds-DNA geometrical diameter, 20 Å).

2. Confirmation of our experimental results in Table 1 for ds-DNA-SAMs assembled on gold under different NaCl concentrations (0.025 ~ 2 M)

(1) Experimentally investigating the relative standard deviation (*RSD*) of experimental data

We investigated the *RSD* of experimental data by choosing two representative assembly NaCl concentrations (lower C_{NaCl}, 0.12 M and higher C_{NaCl}, 2 M) (Table S1) with n = 3. The relative standard deviation (*RSD*) of Γ_m is smaller than 5%, consistent with < 10% from literature [2–6]; the *RSD* of *C* obtained at 0.1 V s^{-1}, $\Phi_{1\ Hz}$ and R_{it}* is about 20%, consistent with the *RSD* values (< 30%) from literature [7,8]; the *RSD* of Δj is < 10% and k_{et} is much bigger and even reaches 46%, which is due to its sensitivity for the defects in SAMs [9–11].

Table S1. Parameters of ds-DNA-SAMs on gold assembled under C_{NaCl} (0.12 and 2 M) (n = 3)

C_{NaCl} (M)	Ions penetration (5 mM phosphate-50 mM NaCl, pH 7.0)								Charge transfer (2 mM $Fe(CN)_6^{3-/4-}$)		Surface coverage
	CV						*EIS*		*CC*	*EIS*	*CC*
	C (μF cm^{-2})						$\Phi_{1\ Hz}$	R_{it}*	Δj	k_{et}	Γ_m
Assembly concentration	0.1 V s^{-1}	0.5 V s^{-1}	1 V s^{-1}	5 V s^{-1}	20 V s^{-1}	50 V s^{-1}	(°)	(Ω cm^2)	(μA cm^{-2})	(cm s^{-1})	(10^{-11} mol cm^{-2})
0.12	18.2 ± 2.9	12.6 ± 2.6	10.8 ± 2.4	7.9 ± 1.9	6.2 ± 1.4	5.5 ± 1.2	73 ± 4	(1.6 ± 0.3) × 10^4	355 ± 34	(1.3 ± 0.6) × 10^{-4}	0.67 ± 0.02
2	35.2 ± 8.7	24.5 ± 5.7	21.0 ± 4.7	15.7 ± 2.7	12.5 ± 1.6	10.9 ± 1.0	75 ± 2	(8.6 ± 2.3) × 10^3	25 ± 1	(1.9 ± 0.3) × 10^{-6}	1.95 ± 0.02

(2) Experimentally cross-checked the experimental data (*C* values) by *CV* and *EIS*

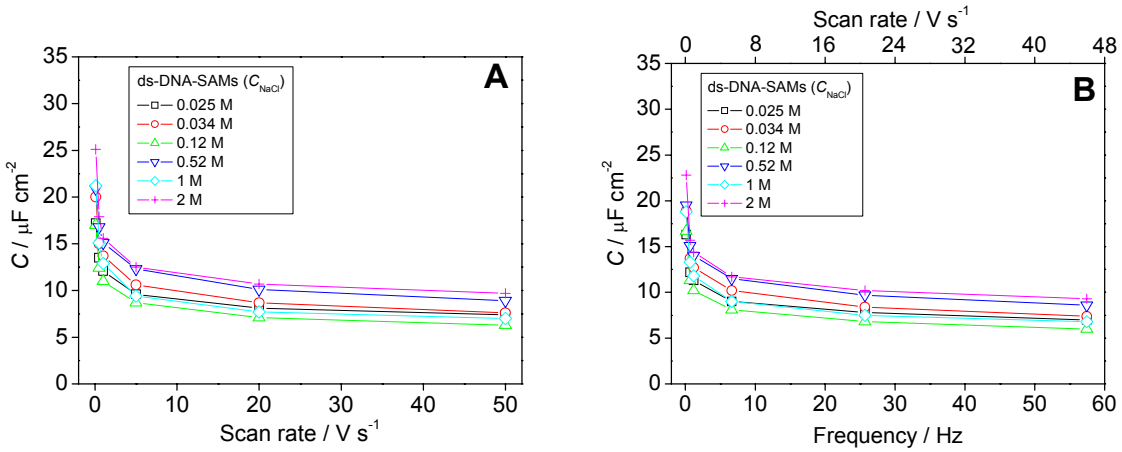

Fig. S2 Relationships of *C* of ds-DNA-SAMs on gold with C_{NaCl} (0.025 ~ 4 M). (A) *C* obtained by *CV* with scan rate *v*; (B) *C* obtained by *EIS* based on the equation $C = \frac{1}{2\pi f_m AZ''}$ with frequency f_m, whereas *Z*'' was the imaginary parts of impedance at the frequency f_m and *A* was the real area of electrode.[12] In order to compare the *C* obtained from *EIS* with *CV*, f_m was designated close to $f_m = \frac{v}{2\Delta E_m} = \frac{v}{2(E_{max} - E_{min})}$ based on the potential zone ($2\Delta E_m = 2(E_{max} - E_{min}) = 0.8$ V) of a *CV* scan period from −0.2 V (E_{min}) to +0.2 V (E_{max}) and scan rate *v* (0.1, 0.5, 1, 5, 20, 50 V s^{-1}). f_m was calculated to be 0.12, 0.66, 1.18, 6.64, 25.7, 57.4 Hz. *Surface coverage Γ_m of ds-DNA-SAMs on gold assembled under different C_{NaCl} (0.025 ~ 2.0 M) was 5×10^{-12}, 6×10^{-12}, 7×10^{-12}, 1.3×10^{-11}, 1.8×10^{-11} and 1.9×10^{-11} mol cm^{-2} from *CC* measurements.

(3) Experimental investigation of ds-DNA-SAMs assembled on gold under different NaCl concentrations (0.025 ~ 2 M) with 5 mM NaH_2PO_4-Na_2HPO_4 (pH 7.0)

In order to further confirm our experimental phenomena (Table 1) for ds-DNA-SAMs formed under different C_{NaCl} (0.025 ~ 2 M) solution, we also assembled ds-DNA on gold under different C_{NaCl} (0.025 ~ 2 M) with 5 mM NaH_2PO_4-Na_2HPO_4 (pH 7.0) and investigated the relationships of parameters (*C*, $\Phi_{1\ Hz}$, R_{it}*, Δj and k_{et}) with C_{NaCl} (Fig. S3 and Table S2). The experimental results proved the experimental phenomena as Table 1 indicated.

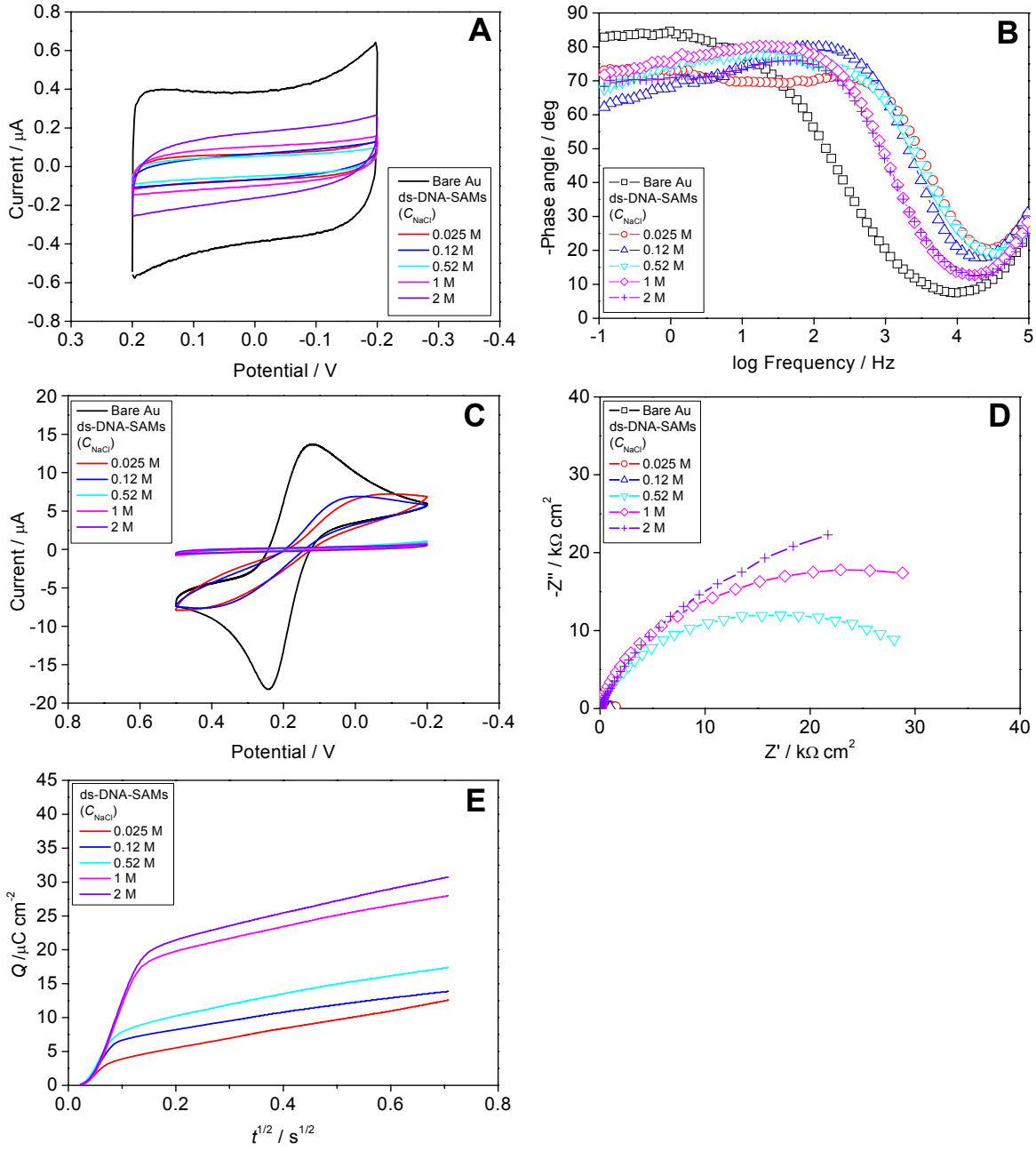

Fig. S3 Electrochemical characteristics of bare Au and ds-DNA-SAMs assembled under different C_{NaCl} (0.025 ~ 2 M) with 5 mM NaH_2PO_4-Na_2HPO_4 (pH 7.0). (A) *CV* plots at 0.1 V s^{-1} and (B) the plots of phase angle with log frequency in blank PBS (5 mM phosphate-50 mM NaCl, pH 7.0) solution; (C) *CV* at 0.1 V s^{-1} and (D) *EIS* plots in 2 mM $Fe(CN)_6^{3-/4-}$ PBS (5 mM phosphate-50 mM NaCl, pH 7.0) solution; (E) *CC* plots (background subtraction) in 50 μM $Ru(NH_3)_6^{3+}$ TBS (10 mM tris-HCl, pH 7.4) solution. The colors of the curves in the figures were: bare Au, black; Assembly C_{NaCl}: 0.025 M, red; 0.12 M, blue; 0.52 M, cyan; 1 M, magenta; 2 M, violet. *Surface coverage Γ_m of ds-DNA-SAMs on gold assembled under different C_{NaCl} (0.025 ~ 2.0 M) with 5 mM NaH_2PO_4-Na_2HPO_4 (pH 7.0) was 3×10^{-12}, 7×10^{-12}, 9×10^{-12}, 1.8×10^{-11} and 1.9×10^{-11} mol cm^{-2} from *CC* measurements.

Table S2. Parameters for characterizing the permeability of ds-DNA-SAMs on gold assembled under different C_{NaCl} (0.025 ~ 2 M) with 5 mM NaH_2PO_4-Na_2HPO_4 (pH 7.0)

C_{NaCl} (M)	Ions penetration (5 mM phosphate-50 mM NaCl, pH 7.0)								Charge transfer (2 mM $Fe(CN)_6^{3-/4-}$)		Surface coverage
	CV C (μF cm^{-2})						*EIS*		*CC*	*EIS*	*CC*
Assembly concentration	0.1 V s^{-1}	0.5 V s^{-1}	1 V s^{-1}	5 V s^{-1}	20 V s^{-1}	50 V s^{-1}	$\Phi_{1\ Hz}$ (^{o})	R_{it}* (Ω cm^2)	Δj (μA cm^{-2})	k_{et} (cm s^{-1})	Γ_m (10^{-11} mol cm^{-2})
0.025	16.3	12.5	10.8	7.2	4.9	3.8	73	1.9×10^4	372	1.2×10^{-4}	0.3
0.12	16.3	10.2	8.4	5.8	4.6	4.4	69	2.0×10^4	357	1.6×10^{-4}	0.7
0.52	12.4	8.7	7.6	5.7	4.7	4.0	75	2.5×10^4	46	4.1×10^{-6}	0.9
1.0	24.8	17.9	15.6	12.1	10.4	9.6	76	1.1×10^4	38	3.3×10^{-6}	1.8
2.0	41.5	28.3	22.7	15.5	11.8	10.4	71	8.2×10^3	30	2.6×10^{-6}	1.9

3. The hexagonal packing of ds-DNA-SAMs on Au(111) with different interaxial distance L_a (n S-S, n = 4 ~ 12) (Ignoring the tilted angle φ)

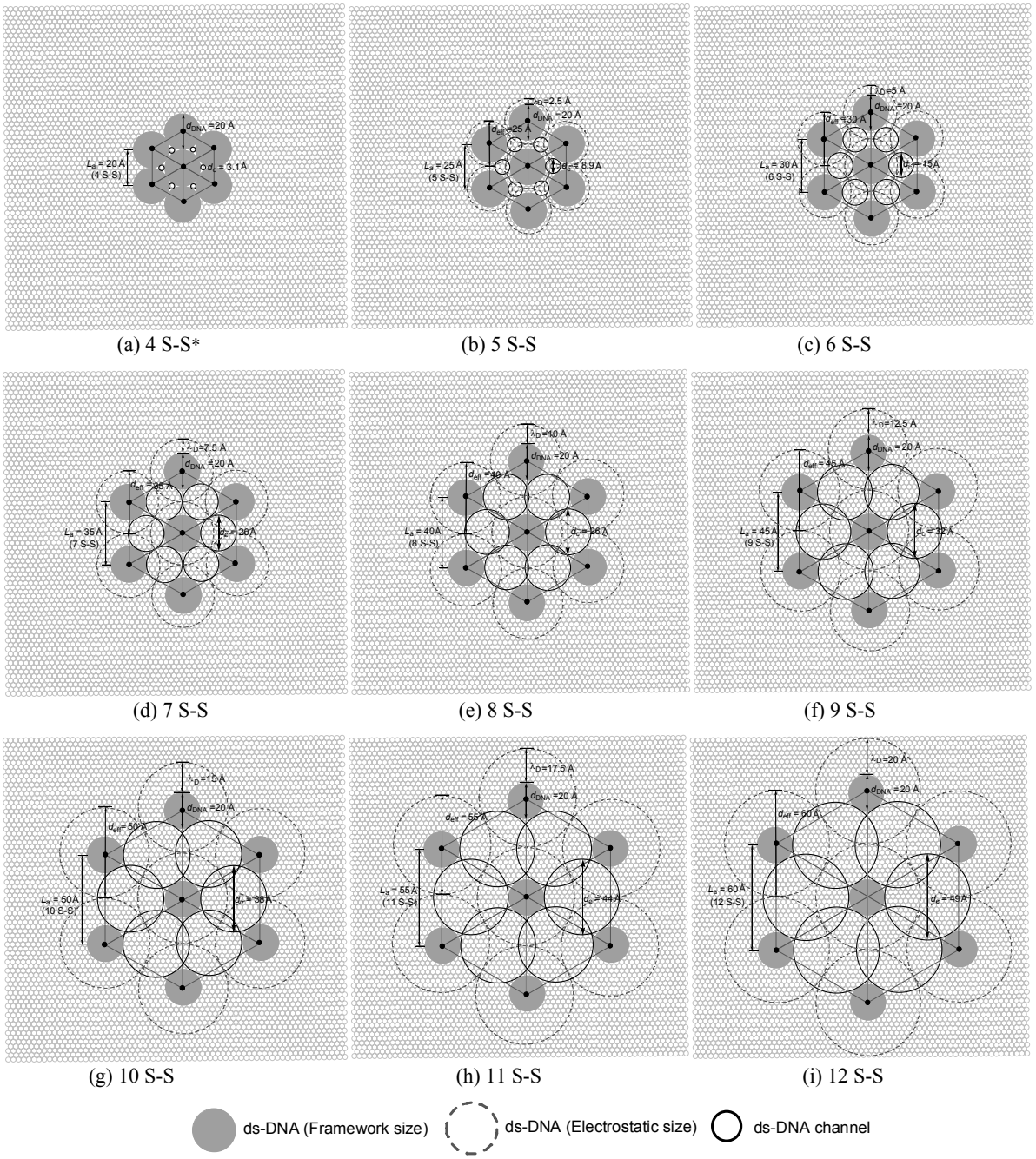

Fig. S4 The hexagonal packing of ds-DNA-SAMs on Au(111) with different interaxial distance L_a for different C_{NaCl} (n S-S, n = 4 ~ 12). *ds-DNA-SAMs with L_a = 20 Å (4 S-S) were impossible due to the existence of repulsive force between adjacent ds-DNA molecules. Three-aggregate channels were the solid circles of adjacent three ds-DNA molecules on Au(111).

4. The hexagonal packing of lying ds-DNA-SAMs on Au(111) with different site distance L_a (n S-S, n = 8 ~ 12) (Tilted angle $\varphi = 90^o$)

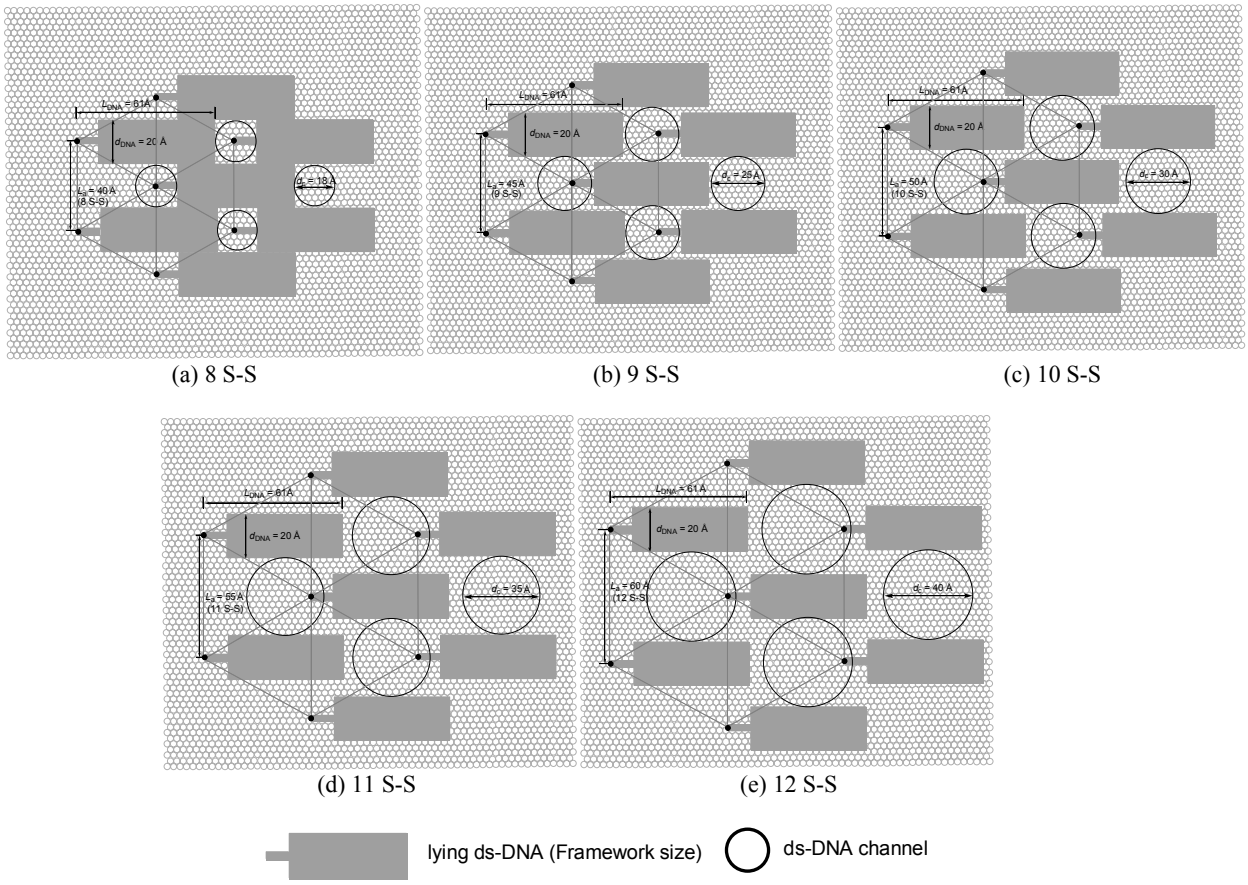

Fig. S5 Simple model for lying ds-DNA-SAMs on Au(111) with different site distance L_a (n S-S, n = 8, 9, 10, 11, 12). Four-aggregate channels were the solid circles of adjacent four ds-DNA molecules on Au(111). The area of joint section (HS-$(CH_2)_6$-) (length 10 Å × width 2.3 Å = 23 Å^2) was much smaller than that of ds-DNA (length 51 Å × width 20 Å = 1020 Å^2), thus, we ignored the joint section (HS-$(CH_2)_6$-) and obtained $S_{DNA} = l_{DNA}\, d_{DNA}$ = 51 × 20 = 1020 Å^2 when calculating the θ_{DNA}* and d_c* in Table 3 based on $\theta_{DNA}{}^{*} = S_{DNA} N_m = \frac{l_{DNA} d_{DNA}}{0.866 L_a{}^2} = \frac{115.5 l_{DNA} d_{DNA}}{L_a{}^2}\%$ $(\varphi = 90^o)$ and $d_c{}^{*} = L_a - d_{DNA}$ $(\varphi = 90^o)$.

5. The change of channel diameter from erecting to tilted ds-DNA-SAMs on Au

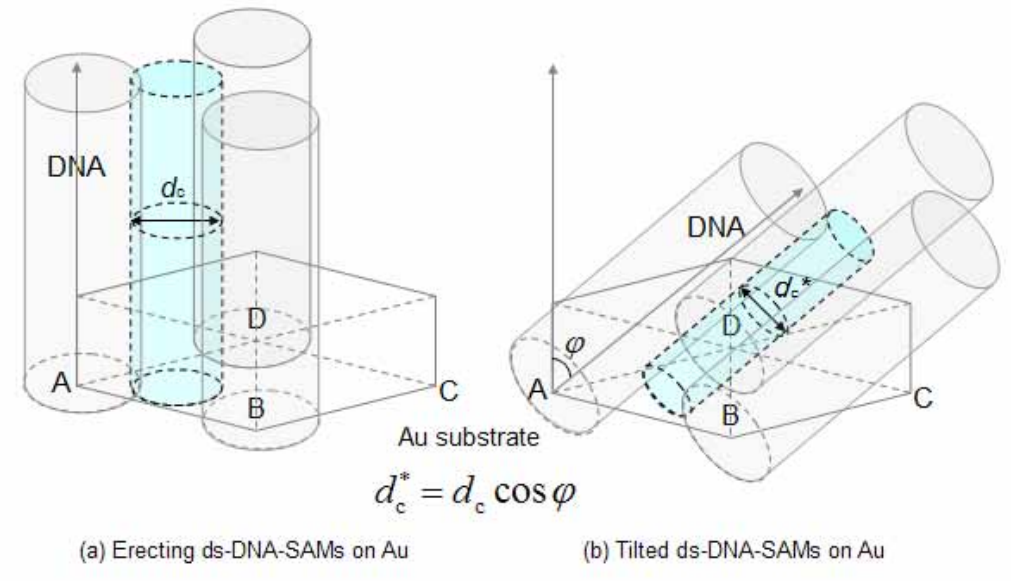

Fig. S6 The change of channel diameter from erecting to tilted ds-DNA-SAMs on Au. The φ is the tilted angle of ds-DNA-SAMs on Au. The channel diameters of erecting and tilted ds-DNA-SAMs are d_c and d_c* respectively with $d_c^* = d_c \cos \varphi$. When the perpendicular interaxial distance a of adjacent tilted ds-DNA molecules (as Fig. S6b showed) was equal to 20 Å, the maximal tilted angle φ_{max} was obtained with $d_c^* = d_c \cos \varphi_{max}$.

6. Confirmation of the data from the model by *CC* experiment and literature reports

Table S3. Interfacial parameters for ds-DNA-SAMs on gold calculated by our proposed model, literature reports and our experimental results[a]

Interfacial parameters for ds-DNA-SAMs on gold calculated by model, literature and our experiment						
			Proposed model[b]			
C_{NaCl} (M)	2	1	0.52	0.12	0.034	0.025
d_{eff} (Å)	24	26	28	38	53	58
L_a (Å)[a]	30 (6 S-S)	30 (6 S-S)	30 (6 S-S)	40 (8 S-S)	55 (11 S-S)	60 (12 S-S)
Γ_m (mol cm^{-2})	2.1×10^{-11}	2.1×10^{-11}	2.1×10^{-11}	1.2×10^{-11}	6.3×10^{-12}	5.3×10^{-12}
φ_{max} (^{o})	59	59	59	90	90	90
			Literature reports[c]			
C_{M^+}(M)		1[13,14]	0.69[15] 0.43[17]		0.055[18]	0.01[2]
Γ_m (mol cm^{-2})		1.8×10^{-11}[13] (*MD*)	1.7×10^{-11}[15] (^{32}P-radiolabeling)		1.3×10^{-12} [18] (^{32}P-radiolabeling)	7.6×10^{-12} [2] (*CV*)
φ (^{o})		45[14] (*NEXAFS*)	51[15] (Ellipsometry) 51~58[17] (Ellipsometry) 65 ~ 72[17] (*AFM*)			
			Our experiment[d]			
C_{NaCl} (M)[c]	2	1	0.52	0.12	0.034	0.025
Γ_m (mol cm^{-2})	1.9×10^{-11}	1.8×10^{-11}	1.3×10^{-11}	7.0×10^{-12}	6.0×10^{-12}	5.0×10^{-12}

*(a) The data difference from the model, literature and our experiment was also perhaps due to the simplification of the model, the difference of experimental conditions or not considering the roughness factor R_f of gold electrodes when calculating the parameters.

(b) Proposed model: C_{NaCl} was the ionic strength for ds-DNA assembly (C_{NaCl} = 0.025 ~ 2 M). d_{eff} was equal to d_{DNA} + 2 λ_D, where λ_D was calculated by Equation 4 in Table 2. L_a was n S-S (1 S-S = 5 Å) and assumed to be the nearest integer of d_{eff} (e.g. for d_{eff} = 28 Å, L_a = 30 Å, 6 S-S) . Γ_m and φ were calculated based on Equation 7 and Equation 12 in Table 2. If considering the hydration force in the model, it was assumed that hydration force dominated the packing of ds-DNA molecules on gold with L_m = 10 Å for $C_{NaCl} \geq$ 0.37 M due to 2 $\lambda_D \leq$ 10 Å [19–22]. Thus, the smallest ds-DNA interaxial distance L_a should be 6 S-S ($d_{DNA} + L_m$ = 20 + 10 = 30 Å) with Γ_m 2.1×10^{-11} mol cm^{-2} for assembly C_{NaCl} (0.52 M, 1 M and 2 M). In this Table, we considered the hydration force when calculating the Γ_m for assembly C_{NaCl} (0.52 M, 1 M and 2 M).

(c) Literature reports: Because cations for ds-DNA self-assembly on gold differed from literatures (e.g. Na^+, K^+), we used C_{M^+} to represent the total concentration of all monovalent cations in assembly solution and did not consider the cations' types. The abbreviation of methods for calculating the Γ_m and φ were in the parentheses: Molecular dynamics simulation (*MD*), Near-edge X-ray absorption fine structure (*NEXAFS*), Atomic force miscropy (*AFM*) and Cyclic voltammetry (*CV*).

Ref. [13]: ds-DNA sequences, 5'-HS-$(CH_2)_6$-$(T)_{25}$-3' with its complementary chain (25 base pairs); Experimental conditions, Molecular dynamics simulation (*MD*) in 1 M NaCl solution; Gold type, Au(111).

Ref. [14]: ds-DNA sequences, 5'-HS–$(CH_2)_6$–TGC AGT TCC GGT GGC TGA TC-SH-3' with its complementary chain (20 base pairs); Assembly conditions: 1 µM ds-DNA in TE buffer (10 mM tris-Cl, 1 mM EDTA, and 1 M NaCl, pH 7.0) for long (>24 h) and short (1 h); Experimental conditions: the φ was from NEXAFS; Au type: gold-coated Si (111) samples (A' and R_f not reported); Pretreatment of gold electrodes: Atomically flat terraces (60 ± 10 nm) separated by facets of 13–15 bunched steps were obtained by a special heating sequence.

Ref. [15]: ds-DNA sequences, 3'-HS-ds-DNA-5' (15 base pairs); Assembly conditions, 50 µM ds-DNA in 0.4 M phosphate buffer (pH 7.2) for 24 h; Experimental conditions, Γ_{DNA} was determined by ^{32}P radioactive labeling and φ was obtained based on the thickness of ds-DNA-SAMs by ellipsometry and L_{DNA} = 57 Å; Gold type, Polycrystalline gold (A' and R_f not reported); Pretreatment of gold electrodes: Gold substrates were placed for 20 min in an ultraviolet ozone cleaner, and then immersed for 20 min in absolute ethanol. Finally, they were rinsed with ethanol [16].

Ref. [17]: ds-DNA sequences, 5'-CTA AGA TTT TCT GCA TAG CAT TAA–TG-3'–$(CH_2)_3$–SH (26 base pairs); Assembly conditions, 15 µM ds-DNA in 25 mM Tris, 0.4 M NaCl for 2~12 h; Experimental conditions, φ was obtained based on the thickness of ds-DNA-SAMs from ellipsometry or AFM and L_{DNA} = 94 Å; Gold type, not mentioned; Pretreatment of gold electrodes: not mentioned.

Ref. [18]: ds-DNA sequences, 5'-TTT TTT TTT TTT TTT-$(CH_2)_6$-SH-3' (15 base pairs); Assembly conditions, 0.1 mM ds-DNA in 5 mM phosphate-50 mM NaCl (pH 7.4) for 18 ~ 48 h; Experimental conditions, Γ_{DNA} was determined by ^{32}P-radiolabeling; Gold type, Au(111) (A' and R_f not reported); Pretreatment of gold electrodes: not mentioned.

Ref. [2]: ds-DNA sequences, HS-$(CH_2)_6$-5'-TCGATCTGACGTCAGCTAAA-3' with its complementary chain (20 base pairs); Assembly conditions, 10 µM ds-DNA in 10 mM tris buffer (pH 7.4) for 18 ~ 48 h; Experimental conditions, Γ_{DNA} was determined by *CV* in 3.5 ~ 12.0 µM $Ru(NH_3)_6^{3+}$/10 mM Tris buffer (pH 7.4); Gold type, evaporated gold films (A' = 0.69 cm^2, R_f not reported); Pretreatment of gold electrodes: Gold substrates were cleaned by immersion in a 3:1 mixture of concentrated H_2SO_4 and 30% H_2O_2 for 5 min at ~ 90 °C and then rinsed with copious amounts of water.

(d) Our experiment: The Γ_m in our experiment was calculated by *CC* experiment in TBS (10 mM tris-HCl, pH 7.4) solution.

7. Electrochemical response of redox probes (negative, positive and neutral) on ds-DNA-SAMs on gold from literature

Table S4. Electrochemical response of redox probes ($Fe(CN)_6^{3-/4-}$, $Ru(NH_3)_6^{3+/2+}$ and Ferrocenemethanol (FcMeOH)) on ds-DNA-SAMs on gold from literature

Amount of base pairs n_{DNA}	Assembly electrolytes	d_c (Å)	d_c* (Å)	φ_{max} (°)	Responses of probes[(a)]	Ref.
	(I) Negatively charged redox probes ($Fe(CN)_6^{3-/4-}$, E^o = 0.12 V)					
	Hydration diameter d_{Hyd} of $Fe(CN)_6^{3-/4-}$ (6.0 Å[29], 9.5 Å[30], ~9 Å[31])					
30	0.1 M phosphate buffer, 1 M NaCl	15 ~ 20	6.5 ~ 7.7	59 ~ 71	×	[23]
20	20 mM tris-ClO_4 (pH 8.6), 0.4 M $NaClO_4$	~26	~4.5	~80	×	[24]
15	5 mM phosphate-50 mM NaCl (pH 7.4)	120	100	~90	×	[18]
20	50 mM tris-ClO_4 (pH 8.7)	~44	~35	~90	×	[25]
20	20 mM tris-ClO_4 (pH 8.7), 20 mM $NaClO_4$	~44	~28	~50	×	[26]
25	20 mM tris-ClO_4 (pH 8.6)	~49	~40	~90	×	[27]
20	0.1 M tris-ClO_4, 0.1 M $NaClO_4$	~38	~30	~90	×	[28]
	(II) Positively charged redox probes ($Ru(NH_3)_6^{3+/2+}$, E^o = –0.19 V)					
	Hydration diameter d_{Hyd} of $Ru(NH_3)_6^{3+/2+}$ (6.4 Å[29], 7.8 Å[32])					
30	0.1 M phosphate buffer, 1 M NaCl	15 ~ 20	6.5 ~ 7.7	59 ~ 71	√	[23]
20	20 mM tris-ClO_4 (pH 8.6), 0.4 M $NaClO_4$	~26	~4.5	~80	√	[24]
20	0.1 M tris-ClO_4, 0.1 M $NaClO_4$	~38	~30	~90	√	[28]
	(III) Neutral redox probe (FeMeOH, E^o = 0.16 V)					
	Hydration diameter d_{Hyd} of FcMeOH (6.8 Å[33])					
20	20 mM tris-ClO_4 (pH 8.6), 0.4 M $NaClO_4$	~26	~4.5	~80	√	[24]

(a) (×) The redox peaks of *CV* and the Warburg line of electrochemical impedance spectroscopy (*EIS*) disappeared indicating that the negatively charged redox probes could not arrive at gold surface and react due to the electrostatic repulsion; (√) Obvious redox peaks of cyclic voltammetry (*CV*) appeared for diffusion-controlled reaction indicating that the positively or neutral redox probes could diffuse to gold surface and react.

(b) The d_c was calculated based on Equation 11 and the d_c* was calculated based on Equation 16 and Equation 17 in Table 2. The φ was reported as 50° for Ref. [26] and the other φ_{max} was calculated based on Equation 12 for $L_a < L_{DNA}/\sqrt{3}$ or Equation 13 for $L_a \geq L_{DNA}/\sqrt{3}$ in Table 2 and the Γ_m values: Ref. [18] was 1.3×10^{-12} mol cm^{-2} from ^{32}P-radiolabeling and the other literature have not reported the Γ_m values, which are roughly estimated by our experimental data of Γ_m in Table 1.

8. List of redox probes to be investigated in our future work

Table S5. List of redox probes

No.	Redox probes	E^o (V vs.SCE)	Size (Å)	
			Framework Size	Van der Waals Size
(a)	Methyl vologen	–0.69	11.3 × 3.4 × 4.9	13.1 × 5.2 × 6.7
(b)	Daunorubicin	–0.60	14.9 × 4.9 × 11.1	16.7 × 6.7 × 12.9
(c)	AQS	–0.46	11.8 × 3.4 × 7.0	13.6 × 5.2 × 8.9
(d)	Methylene blue	–0.23	13.7 × 4.7 × 5.6	15.5 × 6.5 × 7.4
(e)	$Ru(NH_3)_6^{3+/2+}$	–0.19	3.3 × 3.3 × 4.4	5.1 × 5.1 × 6.2
(f)	TMPD	0.03	4.9 × 4.7 × 8.4	6.7 × 6.5 × 10.2
(g)	1, 4-Benzoquinone	0.04	4.9 × 1.5 × 6.8	6.7 × 3.4 × 8.7
(h)	$Fe(CN)_6^{3-/4-}$	0.12	7.4 × 7.4 × 7.4	9.4 × 9.4 × 9.4
(i)	FcMeOH	0.16	6.7 × 4.7 × 5.9	8.5 × 6.5 × 7.8
(j)	Dopamine	0.33	5.9 × 3.6 × 8.6	7.7 × 5.4 × 10.4
(k)	FcDA	0.40	7.3 × 4.7 × 8.2	9.1 × 6.5 × 10.1

*The redox probes with E^o (–0.46 ~ 0.4 V) would be chose to study electron transfer through ds-DNA-SAMs on gold because ds-DNA would be desorbed at potential smaller than –0.60 V in 0.1 M phosphate buffer solution (pH 6.9) by literature reports.[34,35] Anthraquinone-2-sulfonic acid (AQS), N,N,N',N'-Tetramethyl-p-phenylenediamine (TMPD), Ferrocenmethanol (FcMeOH), 1,1'-Ferrocenedicarboxylic acid (FcDA). Framework size from ball-and-stick model of Gaussview software 3.0; Van der Waals size from CPK model of Materials Studio software 3.2.[1] The standard potential E^o: Daunorubicin from literature [36]; Dopamine from literature [37]; FcMeOH from literature [38]; other redox probes from literature [39].

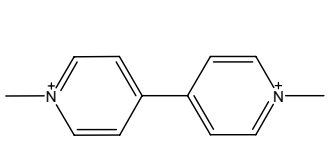

(a) Methyl vologen

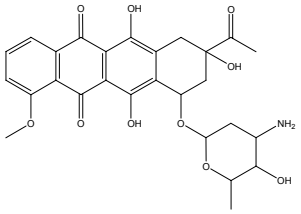

(b) Daunorubicin

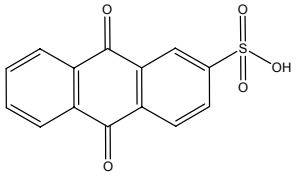

(c) AQS

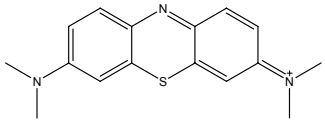

(d) Methylene blue

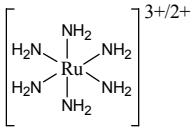

(e) $Ru(NH_3)_6^{3+/2+}$

(f) TMPD

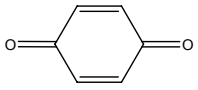

(g) 1, 4-Benzoquinone

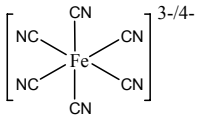

(h) $Fe(CN)_6^{3-/4-}$

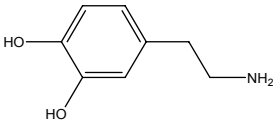

(i) Dopamine

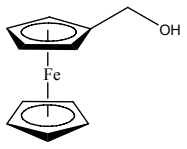

(j) FcMeOH

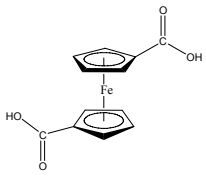

(k) FcDA

9. Derivations of the equations in Table 2 in this article

Table S6. Derivations of the equations in Table 2 in this article

Equations	Derivation of the equations
(1) $\lambda_D = \left(\frac{\varepsilon_0 \varepsilon_r RT}{2F^2 C_{NaCl}}\right)^{1/2}$	The equation was from the literature [40].
(2) $d_{eff} = d_{DNA} + 2\lambda_D$	As Fig. 2A shown that d_{DNA} was the ds-DNA geometrical diameter (20 Å), λ_D was the debye length (Å), d_{eff} was the ds-DNA effective diameter (Å). For example, for ds-DNA under 1 M NaCl solution, λ_D was 3 Å, then, d_{eff} was calculated to be 26 Å.
(3) L_a = n S-S (1 S-S = 5 Å, n = 5, 6, 7, 8…)	As Fig. S4 shown
(4) $L_m = L_a - d_{DNA}$	As Fig. 2A shown
(5) $\Gamma_m = \frac{1}{A_{average} N_A} = \frac{10^{16}}{0.866 N_A L_a^2}$	From the Fig. 2A, the average possessive area (A_{averge}) of each ds-DNA molecule (different from the section area of ds-DNA molecule calculated based on the geometrical diameter d_{DNA} = 20 Å) on Au(111) was equal to the area of parallelogram ABCD. According to the side length of parallelogram ABCD (L_a) and □ABC = 120°, we obtained that A_{averge} = 1/2 (AC × BD) × 10^{-16} where BD = L_a and AC = $\sqrt{3}L_a$. So A = 1/2 × $\sqrt{3}L_a^2$ = 0.866 × 10^{-16} L_a^2 (cm^2). Then Γ_m (mol cm^{-2}) = 10^{16}/0.866 N_A L_a^2.
(6) $N_m = \Gamma_m N_A = \frac{10^{16}}{0.866 L_a^2}$	N_m (molecules cm^{-2}) = $\Gamma_m N_A$ = 10^{16}/0.866L_a^2
(7) $\theta_{DNA} = A_{DNA} N_m = \frac{90.7 d_{DNA}^2}{L_a^2}\%$	The section area of ds-DNA molecule (A_{DNA}) was $A_{DNA} = \pi (d_{DNA}/2)^2 \times 10^{-16}$. According to the amount of ds-DNA molecules each square centimeter (Equation 6, $N_m = \frac{10^{16}}{0.866 L_a^2}$), we obtained $\theta_{DNA} = A_{DNA} N_m \times 100\% = \frac{\pi d_{DNA}^2}{4 \times 0.866 L_a^2} \times 100\% = \frac{90.7 d_{DNA}^2}{L_a^2}\%$.
(8) $N_c = 2N_m = \frac{10^{16}}{0.433 L_a^2}$	Based on Fig. 2A (two channels in parallelogram ABCD), we obtained that the amount of ds-DNA channels N_c was two times as big as that of ds-DNA molecules N_m, so $N_c = 2N_m = 2 \times \frac{10^{16}}{0.866 L_a^2} = \frac{10^{16}}{0.433 L_a^2}$
(9) $d_c = \frac{2}{\sqrt{3}} L_a - d_{DNA} = 1.155 L_a - d_{DNA}$	Based on Fig. S7(a), for ΔAED, AE = DE = $(d_{DNA} + d_c)/2$, AD = L_a, □DAE = 30°, we obtained: $DE^2 = AD^2 + AE^2 - 2\,AD \times AE \cos$□DAE, AD = 2AE cos30° Then L_a = 0.866 ($d_{DNA} + d_c$), we obtained d_c = 1.155 $L_a - d_{DNA}$
(10) $\varphi_{max} = arc\sin\left(1.155\sqrt{1 - 0.866 \times 10^{-16} N_A a^2 \Gamma_m}\right)$ $(L_a = \text{n S} - \text{S} < \frac{L_{DNA}}{\sqrt{3}})$	As shown in Fig. S7(b): (AA', BB' and CC' were the middle axial of tilted ds-DNA molecules; BG□AA', FE□AB, A'F□ABCD; Tilted angle of ds-DNA-SAMs was φ; BG was the perpendicular interaxial distance of adjacent tilted ds-DNA molecules assigned as a, AB and BC were the interaxial distance of adjacent ds-DNA molecules, L_a) Based on A'F□ABCD, we obtained A'F□AB. FE□AB, So AB□ΔA'EF, then AB□A'E. we obtained: cos φ = cos □AA'F = A'F/AA' and sin □A'AE = A'E/AA' Combined the two equation, so sin □A'AE/ cos φ = A'E/A'F. Because $A'E^2 = EF^2 + A'F^2$, EF = AF sin30° = $^1/_2$ AF and tg φ = AF/A'F, we obtained: $A'E^2 = (1 + {}^1/_4 \text{ tg}^2 \varphi)\, A'F^2$ Then sin □A'AE/ cos φ = $\sqrt{1 + \frac{\text{tg}^2\varphi}{4}}$ Because sin □A'AE = sin □GAB = BG/AB = a/ L_a, we obtained: $\frac{a}{L_a \cos\varphi} = \sqrt{1 + \frac{\text{tg}^2\varphi}{4}}$ Then $\sin\varphi = \sqrt{\frac{4}{3}(1 - \frac{a^2}{L_a^2})}$ Based on Equation 5 $\Gamma_m = \frac{10^{16}}{0.866 N_A L_a^2}$, we obtained $L_a^2 = \frac{10^{16}}{0.866 N_A \Gamma_m}$. Then $\sin\varphi_{max} = \sqrt{\frac{4}{3}(1 - 0.866 \times 10^{-16} N_A a^2 \Gamma_m)} = 1.155\sqrt{1 - 0.866 \times 10^{-16} N_A a^2 \Gamma_m}$ $\varphi_{max} = \arcsin\left(1.155\sqrt{1 - 0.866 \times 10^{-16} N_A a^2 \Gamma_m}\right)$ (a = 20 Å)

Table S6. Derivations of the equations in Table 2 in this article (continued)

Equations	Derivation of the equations
(11) $\varphi = 90^{\circ} \quad (L_a = \mathrm{n\,S - S} \geq \frac{L_{DNA}}{\sqrt{3}})$	As Fig. 2B and Fig. S5 shown, ds-DNA could lie flat on gold for $L_{AC} \geq L_{DNA}$. Based on $L_{AC} = \sqrt{3}\,L_a$, we obtained $L_a = \mathrm{n\,S - S} \geq \frac{L_{DNA}}{\sqrt{3}}$.
(12) $\theta_{DNA}* = S_{DNA}N_m = \frac{l_{DNA}d_{DNA}}{0.866L_a^{\,2}} = \frac{115.5l_{DNA}d_{DNA}}{L_a^{\,2}}\% \quad (\varphi = 90^{\circ})$	As Fig. S5 shown, the area of ds-DNA molecule lying on gold was $S_{DNA} = l_{DNA}d_{DNA} \times 10^{-16}\,\mathrm{cm}^2$ and the ds-DNA surface coverage was $N_m = 10^{16}/0.866L_a^{\,2}$ molecules cm^{-2}. Then $\theta_{DNA}* = S_{DNA}N_m = \frac{l_{DNA}d_{DNA}}{0.866L_a^{\,2}} = \frac{115.5l_{DNA}d_{DNA}}{L_a^{\,2}}\% \quad (\varphi = 90^{\circ})$
(13) $N_c* = \Gamma_m = \frac{10^{16}}{0.866L_a^{\,2}} \quad (\varphi = 90^{\circ})$	As Fig. S5 shown
(14) $d_c* = (1.155L_a - d_{DNA})\cos\varphi \quad (0^{\circ} < \varphi < 90^{\circ})$	When ds-DNA tilted with the angle ($0^{\circ} < \varphi < 90^{\circ}$), based on Fig. 2B, $d_c = (1.155\,L_a - d_{DNA})\cos\varphi$.
(15) $d_c* = L_a - d_{DNA} \quad (\varphi = 90^{\circ})$	When ds-DNA lied flat ($\varphi = 90^{\circ}$), based on Fig. S5, $d_c* = L_a - d_{DNA}$.

*Meanings of parameters in the equations and units: λ_D (debye length, Å), d_{eff} (ds-DNA effective diameter, Å), L_a (ds-DNA interaxial distance, Å), L_m (ds-DNA marginal distance, Å), Γ_m (ds-DNA surface coverage, mol cm^{-2}), N_m (ds-DNA surface coverage, molecules cm^{-2}), θ_{DNA} (area ratio of ds-DNA cross section with gold surface), d_c (channel diameter, Å), N_c (amount of ds-DNA channels, channels cm^{-2}), φ (tilted angle of ds-DNA-SAMs, °), $\theta_{DNA}*$ (ds-DNA area percentage on gold surface, $\varphi = 90^{\circ}$), d_c* (channel diameter, Å, $\varphi = 90^{\circ}$), N_c* (channel amount, channels cm^{-2}, $\varphi = 90^{\circ}$), R (gas constant, 8.314 J $\mathrm{mol}^{-1}\,\mathrm{K}^{-1}$), T (temperature, K), F (Faraday constant, 96485 C mol^{-1}), C_{NaCl} (NaCl concentration, M), ε_o (the permittivity of free space, $8.85 \times 10^{-14}\,\mathrm{C}^2\,\mathrm{J}^{-1}\,\mathrm{cm}^{-1}$), ε_r (the dielectric constant of water, 78), L_{DNA} (the geometrical length of thiol-modified ds-DNA molecule, 61 Å in this study), l_{DNA} (ds-DNA geometrical length, 51 Å in this study), d_{DNA} (ds-DNA geometrical diameter, 20 Å), A_{averge} (the average possessive area of each ds-DNA molecule on Au(111) which was equal to the area of parallelogram ABCD (Fig. 2A), $A_{averge} = \sqrt{3}/2 \times 10^{-16} L_a^{\,2}\,\mathrm{cm}^2$), A_{DNA} (area of ds-DNA section, $A_{DNA} = \pi\,(d_{DNA}/2)^2 \times 10^{-16}\,\mathrm{cm}^2$), S_{DNA} (area of lying ds-DNA on Au(111), $S_{DNA} = l_{DNA}d_{DNA} \times 10^{-16}\,\mathrm{cm}^2$), N_A (Avogadro constant, $6.02 \times 10^{23}\,\mathrm{mol}^{-1}$), a (the perpendicular interaxial distance of adjacent tilted ds-DNA molecules, a ≥ 20 Å), 1 S-S was the distance (5 Å) of adjacent hollow sites (f_{cc}) on Au(111).

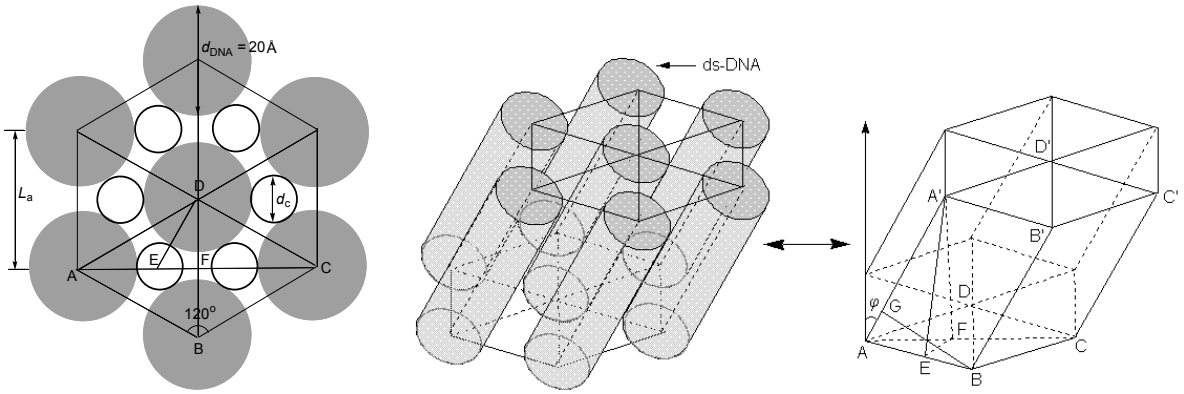

(a) Planform (b) Stereogram

Fig. S7 Planform and stereogram of ds-DNA-SAMs on Au(111).

10. References

1 Accelrys Software Inc. Material Studio Modeling 3.2, San Diego, USA. 2004.

2 H. Z. Yu, C. Y. Luo, C. G. Sankar and D. Sen, *Anal. Chem.*, 2003, **75**, 3902–3907.

3 R. Meunier-Prest, A. Bouyon, E. Rampazzi, S. Raveau, P. Andreoletti and M. Cherkaoui-Malki, *Biosens. Bioelectron.*, 2010, **25**, 2598–2602.

4 A. B. Steel, R. L. Levicky, T. M. Herne and M. J. Tarlov, *Biophys. J.*, 2000, **79**,

975–981.

5 X. D. Su, Y. J. Wu, R. Robelek and W. Knoll, *Langmuir*, 2005, **21**, 348–353.

6 W. C. Liao and J. A. Ho, *Anal. Chem.*, 2009, **81**, 2470–2476.

7 M. Tichoniuk, D. Gwiazdowska, M. Ligaj and M. Filipiak, *Biosens. Bioelectron.*, 2010, **26**, 1618–1623.

8 A. B. Steel, T. M. Herne and M. J. Tarlov, *Anal. Chem.*, 1998, **70**, 4670−4677.

9 Z. G. Li, T. X. Niu, Z. J. Zhang and S. P. Bi, *Electrochim. Acta*, 2010, **55**, 6907−6916.

10 L. V. Protsailo, W. R. Fawcett, D. Russell and R. L. Meyer, *Langmuir*, 2002, **18**, 9342–9349.

11 R. D. Weinstein, J. Moriarty, E. Cushnie, R. Colorado, T. R. Lee, M. Patel, W. R. Alesi and G. K. Jennings, *J. Phys. Chem. B*, 2003, **107**, 11626–11632.

12 W. O. Ho, S. Krause, C. J. McNeil, J. A. Pritchard, R. D. Armstrong, D. Athey and K. Rawson, *Anal. Chem*., 1999, **71**, 1940–1946.

13 L. Q. Yao, J. Sullivan, J. Hower, Y. He and S. Y. Jiang, *J. Chem. Phys*., 2007, **127**, 195101(1–6).

14 J. N. Crain, A. Kirakosian, J. L. Lin, Y. D. Gu, R. R. Shah, N. L. Abbott and F. J. Himpsela, *J. Appl. Phys.*, 2001, **90**, 3291–3295.

15 R. Naaman and Z. Vager, *Phys. Chem. Chem. Phys*., 2006, **8**, 2217−2224.

16 T. Aqua, R. Naaman and S. S. Daube, *Langmuir*, 2003, **19**, 10573−10580.

17 H. Cohen, C. Nogues, D. Ullien, S. Daube, R. Naaman and D. Porath, *Faraday Discuss.*, 2006, **131**, 367–376.

18 R. Meunier-Prest, S. Raveau, E. Finot, G. Legay, M. Cherkaoui-Malki and N. Latruffe, *Nucleic Acids Res.*, 2003, **31**, e150 (1 –8).

19 D. C. Rau and V. A. Parsegian, *Biophys. J*., 1992, **61**, 260–271.

20 R. Podgornik, D. C. Rau and V. A. Parsegian, *Macromolecules*, 1989, **22**, 1780–1786.

21 K. Castelino, B. Kannan and A. Majumdar, *Langmuir*, 2005, **21**, 1956–1961.

22 J. Mertens, C. Rogero, M. Calleja, D. Ramos, J. A. Martin-Gago, C. Briones and J. Tamayo, *Nat. Nanotech*., 2008, **3**, 301–307.

23 P. C. J. Jian, T. F. Liu, C. M. Tsai, M. S. Tsai and C. C. Chang, *Nanotechnology*, 2008, **19**, 355703 (1–8).

24 B. Liu, A. J. Bard, C. Z. Li and H. B. Kraatz, *J. Phys. Chem. B*, 2005, **109**, 5193–5198.

25 X. H. Li, J. S. Lee and H. B. Kraatz, *Anal. Chem.*, 2006, **78**, 6096–6101.

26 Y. T. Long, C. Z. Li, H. B. Kraatz and J. S. Lee, *Biophys. J.*, 2003, **84**, 3218–3225.

27 X. M. Bin and H. B. Kraatz, *Analyst*, 2009, **134**, 1309–1313.

28 C. Z. Li, Y. T. Long, H. B. Kraatz and J. S. Lee. *J. Phys. Chem. B*, 2003, **107**, 2291–2296.

29 O. Chailapakul and R. M. Crooks, *Langmuir*, 1995, **11**, 1329–1340.

30 F. Fornasiero, H. G. Park, J. K. Holt, M. Stadermann, C. P. Grigoropoulos, A. Noy and O. Bakajin, *Proc. Natl. Acad. Sci. USA*, 2008, **105**, 17250–17255.

31 J. G. Speight, Lange's Handbook of Chemistry, 16th ed. McGraw-Hill, Inc., New York, 2005.

32 J. T. Surek and D. D. Thomas, *J. Magn. Reson.*, 2008, **190**, 7–25.

33 M. P. Longinotti and H. R. Corti, *Electrochem. Commun.*, 2007, **9**, 1444–1450.

34 H. Wackerbarth, M. Grubb, J. D. Zhang, A. G. Hansen and J. Ulstrup, *Langmuir*, 2004, **20**, 1647–1655.

35 H. Wackerbarth, M. Grubb, J. Wengel, I. Chorkendorff and J. Ulstrup, *Surf. Sci.*, 2006, **600**, 122–127.

36 L. X. Cao, P. S. Yan, K. N. Sun and D. W. Kirk, *Electroanalysis*, 2009, **21**, 1183–1188.

37 H. M. Zhang, N. Q. Li and Z. W. Zhu, *Microchem. J.,* 2000, **64**, 277–282.

38 A. K. Neufeld and A. P. O'Mullane, *J. Solid State Electrochem.*, 2006, **10**, 808–816.

39 (a) A. J. Bard, J. Jordan and R. Parsons, Strandard Potentials in Aqueous Solution, Marcel Dekker, New York, 1985; (b) W. Clark, Oxidation-Reduction Potentials of Organic Systems. Williams & Wilkins Co. Baltimore, 1960; (c) M. L. Fultz, R. A. Durst, *Anal. Chim. Acta*, 1982, **140**, 1–18; (d) P. N. Bartlett, P. Tebbutt and R. G. Whitaker, *Prog. Reaction Kinetics*, 1991, **16**, 55–155; (e) R. Szentrimay, P. Yeh and T. Kuwana, Electrochemical Studies of Biological Systems, ACS, Washington, DC 1977.

40 R. Tadmor, E. Hernandez-Zapata, N. H. Chen, P. Pincus and J. N. Israelachvili, *Macromolecules*, 2002, **35**, 2380−2388.